

# Testing the nuclear TMD gluon densities with heavy flavor production in proton-lead collisions at LHC

A.V. Lipatov<sup>1</sup>, A.V. Kotikov<sup>2</sup>

February 10, 2026

<sup>1</sup>*Skobeltsyn Institute of Nuclear Physics, Lomonosov Moscow State University, 119991 Moscow, Russia*

<sup>2</sup>*Joint Institute for Nuclear Research, 141980 Dubna, Moscow region, Russia*

## Abstract

We employ a simple model for nuclear modification of ordinary parton densities in a proton to evaluate the Transverse Momentum Dependent gluon and quark distributions in nuclei (nTMDs) within the popular Kimber-Martin-Ryskin/Watt-Martin-Ryskin approach. The model is based on a global analysis of available deep inelastic scattering data for different nuclear targets within the rescaling model, incorporating Fermi motion effects. The derived nTMDs are tested with latest CMS data on inclusive  $b$ -jet and  $B^+$  meson production in proton-lead collisions collected at  $\sqrt{s} = 5.02$  and  $8.16$  TeV using the High Energy Factorization framework. We predict the corresponding nuclear medium modification factors to be about of  $0.8 - 1.2$  in the probed kinematical region, which is consistent with other estimations. Specially we highlight a possibility to investigate the nuclear modification of parton densities by applying different cuts on the final states in such processes.

*Keywords:* small- $x$  physics, parton densities in a proton and nuclei, heavy flavor production

It is known that, at present, any theoretical investigation of QCD processes is usually relies on a factorization of the effects of short and long distances at some scale. A key ingredient of such consideration is the parton (gluon and quark) distribution functions in a proton (PDFs),  $f_a(x, \mu^2)$  with  $a = g$  or  $q$  and  $x$  being the longitudinal momentum fraction of proton carried by parton  $a$ , which describe the parton content of a proton at the scale  $\mu^2$ . In the conventional QCD factorization, the PDFs obey the Dokshitzer-Gribov-Lipatov-Altarelli-Parisi (DGLAP) equations [1]. At high energies, an alternative description can be achieved within the High Energy Factorization [2], or  $k_T$ -factorization approach [3], which is based on the Balitsky-Fadin-Kuraev-Lipatov (BFKL) [4] or Catani-Ciafaloni-Fiorani-Marchesini (CCFM) [5] evolution equations for transverse momentum dependent (TMD, or unintegrated) gluon densities in a proton,  $f_g(x, \mathbf{k}_T^2, \mu^2)$ . Such an approach has certain technical advantages in the ease of including higher-order radiative corrections corresponding to the gluon emissions in the initial state (see, for example, reviews [6, 7] for more information).

When it comes to nuclei, a number of complications arise. As is known, the nucleus is far from a simple picture of quasi-free nucleons [8–11]. Instead one finds so-called nuclear shadowing, anti-shadowing, EMC effect and Fermi motion dominance regions at  $x \leq 0.1$ ,  $0.1 \leq x \leq 0.3$ ,  $0.3 \leq x \leq 0.7$  and  $x \geq 0.7$ , respectively. Defining the nuclear medium modification factor as a ratio of per-nucleon deep inelastic structure functions in nuclei  $A$  and deuteron  $R_{AD} = F_2^A(x, Q^2)/F_2^D(x, Q^2)$ , one then can refer to the shadowing and anti-shadowing effects as having  $R_{AD} < 1$  and  $R_{AD} > 1$ , whereas EMC effect and Fermi motion correspond to a drop of  $R_{AD}$  in the valence-dominant region and an increasing of  $R_{AD}$  at larger  $x$ . So, corresponding pQCD calculations demand nuclear PDFs and/or TMDs (nPDFs or nTMDs), which essentially differ from the usual parton distributions in a proton. Of course, their detailed knowledge — in particular, knowledge of nuclear gluon densities — is necessary for any theoretical description and proper interpretation of  $pA$  processes studied at modern (LHC, RHIC) and future colliders (FCC-he, EiC, EicC, NICA). In turn,  $pA$  collisions is a natural reference for more complex nucleus-nucleus ( $AA$ ) interactions, where nuclear matter can reach extremely high energy densities and temperatures, transforming into its hot and dense deconfined phase, the quark-gluon plasma (QGP) [12, 13].

Despite significant theoretical efforts made in recent years, nPDFs and especially nTMDs are still poorly known at present and have large uncertainties due to shortage of experimental data and/or their limited kinematic coverage (see [14–16] and references therein). Several approaches could be used to evaluate these objects. In fact, they could be extracted from a global fit to nuclear data and then their scale dependence can be determined as a solution of QCD evolution equations (see, for example, [17–20] for nPDFs and [21] for nTMDs). This technique is in a close analogy with the standard derivation of the PDFs and/or TMDs. The second strategy is based on special models [22–27], in particular, rescaling model [24, 25] and approaches where the geometrical scaling [26, 27] is applied [28, 29]. So, in the rescaling model it is assumed that the effective size of gluon and quark confinement in the nucleus is greater than in the free nucleon, thus giving a shift in the hard scale  $\mu^2$  (see also review [30]).

In this note, we concentrate mainly on the nTMD gluon densities and derive them from nPDFs using the popular Kimber-Martin-Ryskin (KMR) [31] or Watt-Martin-Ryskin (WMR) [32] approach. The WMR prescription is an extension and further development of KMR formalism and explored currently at the next-to-leading order (NLO) [33]. In the KMR/WMR method, the DGLAP strong ordering condition is relaxed at the last step of parton evolution cascade, so the transverse momentum is no longer negligible compared to the evolution scale  $\mu^2$ , thus giving rise to the transverse momentum dependence of

the parton densities. Such prescription, where ordinary PDFs are employed as an input for the KMR/WMR procedure, is widely used in phenomenological applications (see, for example, [34–39] and references therein). The KMR/WMR method to generate nTMDs has been used already [40, 41]. So, the analytical leading order (LO) expressions [42–44] (see also [45, 46]) for PDFs obtained at small  $x$  in the generalized double asymptotic scaling approximation [47–49] have been extended to nPDFs using the rescaling model adopted for low  $x$  [44] and then applied as an input for the KMR/WMR formulas [41].

Recently, an early derivation [42–44] was significantly improved by taking into account the exact asymptotics at low and large  $x$  and by incorporating subasymptotic terms fixed by the momentum conservation and/or Gross-Llewellyn-Smith and Gottfried sum rules [50, 51]. Moreover, a simple model for nuclear modification of these improved PDFs has been proposed very recently [52]. The approach [52] is based on the global analysis of available deep inelastic scattering data for different nuclear targets within the low- $x$  enhanced rescaling model combined with the effects of Fermi motion. Here we employ the KMR/WMR formalism to calculate nTMDs within the proposed model [52]. Then, we will test the derived TMDs with inclusive beauty production in  $pA$  collisions at the LHC. Such processes are known to be sensitive to the gluon content of the nucleus and provide us with a possibility to reconstruct the full map of the latter (see, for example, [53]). Moreover, they provide a unique opportunity to study the QGP [54, 55]. In fact, by studying how the nuclear medium affects heavy quarks, the properties of the medium can be determined. Using the Monte-Carlo event generator PEGASUS [56], which implements now the TMD gluon dynamics in nuclei, we calculate the transverse momentum and rapidity distributions of  $b$ -jets and  $B^+$  mesons and compare our predictions with latest experimental data [57–59] collected by the CMS Collaboration at  $\sqrt{s} = 5.02$  and 8.16 TeV. Of course, these data are of a great importance to test the derived predictions for nTMDs. Then we investigate corresponding effects of nuclear medium modifications in different kinematical regions. The consideration below extends and continues the line of our previous studies [41, 44, 52].

We start from a very brief description of our approach. In the fixed-flavor-number-scheme (FFNS) with  $N_f = 4$ , where  $b$  and  $t$  quarks are separated out, the non-singlet ( $NS$ ) and valence ( $V$ ) parts of quark distribution functions at the LO can be represented in the following form [51]:

$$f_i(x, \mu^2) = \left[ A_i(s) x^{\lambda_i} (1-x) + \frac{B_i(s) x}{\Gamma(1 + \nu_i(s))} + D_i(s) x(1-x) \right] (1-x)^{\nu_i(s)}, \quad (1)$$

where  $i = NS$  or  $V$ ,  $s = \ln [\alpha_s(\mu_0^2)/\alpha_s(\mu^2)]$  and

$$\begin{aligned} A_i(s) &= A_i(0) e^{-d(n_i)s}, & B_i(s) &= B_i(0) e^{-ps}, & \nu_i(s) &= \nu_i(0) + rs, \\ r &= \frac{16}{3\beta_0}, & p &= r(\gamma_E + \hat{c}), & \hat{c} &= -\frac{3}{4}, & d(n) &= \frac{\gamma_{NS}(n)}{2\beta_0}, & n_i &= 1 - \lambda_i. \end{aligned} \quad (2)$$

Here  $\Gamma(z)$  is the Riemann's  $\Gamma$ -function,  $\gamma_E \simeq 0.5772$  is the Euler's constant,  $\beta_0 = 11 - 2N_f/3$  is the LO QCD  $\beta$ -function,  $\lambda_{NS} = \lambda_V = 0.5$ ,  $\gamma_{NS}(n)$  is the LO non-singlet anomalous dimension and  $A_i(0)$ ,  $B_i(0)$  and  $\nu_i(0)$  are the free parameters. The term proportional to  $D_i(s)$  is a subasymptotic one and its scale dependence is fixed by the Gross-Llewellyn-Smith and Gottfried sum rules [51]:

$$D_i(s) = (2 + \nu_i(s)) \left[ N_i - A_i(s) \frac{\Gamma(\lambda_i) \Gamma(2 + \nu_i(s))}{\Gamma(\lambda_i + 2 + \nu_i(s))} - \frac{B_i(s)}{\Gamma(2 + \nu_i(s))} \right], \quad (3)$$

where  $N_V = 3$  and  $N_{NS} \equiv I_G(\mu^2) = 0.705 \pm 0.078$  (see [51] and references therein for more information). The singlet ( $SI$ ) part of quark densities and gluon distribution in a

proton can be represented as combinations of "±" terms (see also [42–44]):

$$f_i(x, \mu^2) = f_i^+(x, \mu^2) + f_i^-(x, \mu^2), \quad (4)$$

where  $i = SI$  or  $g$  and

$$f_{SI}^+(x, \mu^2) = \left[ \frac{N_f}{9} \left( A_g + \frac{4}{9} A_q \right) \rho I_1(\sigma) e^{-\bar{d}^+ s} (1-x)^{m_q^+} + D^+(s) \sqrt{x} (1-x)^{n^+} - \frac{K^+}{\Gamma(2 + \nu^+(s))} \times \frac{B^+(s)x}{\hat{c} - \ln(1-x) + \Psi(2 + \nu^+(s))} \right] (1-x)^{\nu^+(s)+1}, \quad (5)$$

$$f_{SI}^-(x, \mu^2) = \left[ A_q e^{-d^- s} (1-x)^{m_q^-} + \frac{B^-(s)x}{\Gamma(1 + \nu^-(s))} + D^-(s) \sqrt{x} (1-x)^{n^-} \right] (1-x)^{\nu^-(s)}, \quad (6)$$

$$f_g^+(x, \mu^2) = \left[ \left( A_g + \frac{4}{9} A_q \right) I_0(\sigma) e^{-\bar{d}^+ s} (1-x)^{m_g^+} + \frac{B^+(s)x}{\Gamma(1 + \nu^+(s))} \right] (1-x)^{\nu^+(s)}, \quad (7)$$

$$f_g^-(x, \mu^2) = \left[ -\frac{4}{9} A_q e^{-d^- s} (1-x)^{m_g^-} + \frac{K^-}{\Gamma(2 + \nu^-(s))} \times \frac{B^-(s)x}{\hat{c} - \ln(1-x) + \Psi(2 + \nu^-(s))} \right] (1-x)^{\nu^-(s)+1}. \quad (8)$$

Here  $\Psi(z)$  is the Riemann's  $\Psi$ -function,  $I_0(z)$  and  $I_1(z)$  are the modified Bessel functions and

$$\begin{aligned} \nu^\pm(s) &= \nu^\pm(0) + r^\pm s, \quad B^\pm(s) = B^\pm(0) e^{-p^\pm s}, \quad p^\pm = r^\pm(\gamma_E + \hat{c}^\pm), \\ r^+ &= \frac{12}{\beta_0}, \quad r^- = \frac{16}{3\beta_0}, \quad \hat{c}^+ = -\frac{\beta_0}{12}, \quad \hat{c}^- = -\frac{3}{4}, \quad K^+ = \frac{3N_f}{10}, \quad K^- = \frac{2}{5}, \\ \rho &= \frac{\sigma}{2 \ln(1/x)}, \quad \sigma = 2 \sqrt{|\hat{d}^+| s \ln \frac{1}{x}}, \\ \hat{d}^+ &= -\frac{12}{\beta_0}, \quad \bar{d}^+ = 1 + \frac{20N_f}{27\beta_0}, \quad d^- = \frac{16N_f}{27\beta_0} \end{aligned} \quad (9)$$

with  $A_g$ ,  $A_q$ ,  $B^\pm(0)$ ,  $\nu^\pm(0)$ ,  $m_q^\pm$ ,  $m_g^\pm$  and  $n^\pm$  being free parameters. The expressions for subasymptotic terms  $D^\pm(s)$  were derived from the momentum conservation law and could be found elsewhere [51]. All the parameters in the formulas above have been determined from a rigorous fit to precision BCDMS, H1 and ZEUS experimental data on the proton structure function  $F_2(x, Q^2)$  in a wide kinematical region,  $2 \cdot 10^{-5} \leq x \leq 0.75$  and  $1.2 \leq Q^2 \leq 30000$  GeV $^2$  [51]. A perfect goodness of the fit<sup>1</sup>,  $\chi^2/n.d.f. = 1.408$ , was achieved.

Our next step is connected with nuclear modifications of derived PDFs. The combination of the rescaling model extended to low  $x$  (or shadowing region) and Fermi motion was applied [52]. So, for a nucleus  $A$ , the valence and nonsinglet parts are modified as:

$$f_i^A(x, \mu^2) = f_i(x, \mu_{A,i}^2), \quad (10)$$

---

<sup>1</sup>The fit was comprising a total of 933 points from 5 data sets.

where  $i = V$  or  $NS$  and scale  $\mu_{A,i}^2$  is related to  $\mu^2$  by:

$$s_i^A \equiv \ln \left( \frac{\ln (\mu_{A,i}^2 / \Lambda_{\text{QCD}}^2)}{\ln (\mu_0^2 / \Lambda_{\text{QCD}}^2)} \right) = s + \ln (1 + \delta_i^A), \quad (11)$$

with  $\delta_i^A$  being the scale independent free parameters (see [44] and references therein) and analytical expressions for  $f_i(x, \mu^2)$  are given by (1) — (3). For singlet quark and gluon parts which have two ('+' and '−') independent components, one has two additional rescaling parameters  $\delta_{\pm}^A$  (see [44]). So,

$$f_i^A(x, \mu^2) = f_i^{A,+}(x, \mu^2) + f_i^{A,-}(x, \mu^2), \quad f_i^{A,\pm}(x, \mu^2) = f_i^{\pm}(x, \mu_{A,\pm}^2), \quad (12)$$

where  $i = SI$  or  $g$  and expressions for  $f_i^{\pm}(x, \mu^2)$  are given by (4) — (9). The definition of  $\mu_{A,\pm}^2$  is the same as above and corresponding values of  $s_{\pm}^A$  turned out to be [44]

$$s_{\pm}^A \equiv \ln \left( \frac{\ln (\mu_{A,\pm}^2 / \Lambda_{\text{QCD}}^2)}{\ln (\mu_0^2 / \Lambda_{\text{QCD}}^2)} \right) = s + \ln (1 + \delta_{\pm}^A). \quad (13)$$

where the free parameters  $\delta_{\pm}^A$  are scale independent and have to be negative.

The full model [52] takes into account the effects of Fermi motion of nucleons inside the nuclear target. These effects deform the nuclear structure functions mainly at large  $x > 0.7$ . Such deformation could be described by the convolution [60, 61]:

$$f_i^{A(F)}(x, \mu^2) = \frac{1}{R_i} \int \frac{dy}{y} [y f_N(y)] f_i^A(x/y, \mu^2), \quad (14)$$

where  $i = V, NS, SI$  or  $g$ . The expressions for  $f_N(y)$  and  $R_i$  can be found elsewhere [52]. The rescaling parameters  $\delta_V^A, \delta_{NS}^A$  and  $\delta_{\pm}^A$  have been extracted [52] from the global fit on experimental data on structure function ratios  $F_2^A(x, Q^2)/F_2^{A'}(x, Q^2)$  for various nuclear targets  $A$  and  $A'$  in the deep inelastic region. Moreover, their nuclear dependence was investigated and parametrized in several ways, which are often assumed in the literature (see, for example, [19, 62–68] and references therein):  $\delta_i^A \sim A^{1/3}$  (Fit A),  $\delta_i^A \sim \ln A$  (Fit B) and  $\delta_i^A \sim A^{1/3} + A^{-1/3}$  (Fit C). Thus, within the model [52], the nuclear medium modification factor  $R$  can be calculated for any nucleus, even for unmeasured ones.

Now we are able to calculate the nTMDs using the approach [52] and LO KMR/WMR formalism. There are known differential and integral definitions of the latter (see discussions [69–72]). Here we employ the integral definition, which is more preferable<sup>2</sup> in the phenomenological applications [69]. In this way, the nTMDs could be written as

$$f_a^A(x, \mathbf{k}_T^2, \mu^2) = T_a(\mathbf{k}_T^2, \mu^2) \frac{\alpha_s(\mathbf{k}_T^2)}{2\pi \mathbf{k}_T^2} \sum_b \int_x^{1-\Delta} dz P_{ab}(z) f_b^{A(F)}\left(\frac{x}{z}, \mathbf{k}_T^2\right), \quad (15)$$

where  $a = q$  or  $g$ ,  $P_{ab}(z)$  are the usual unregulated LO DGLAP splitting functions and  $\Delta$  is some cutoff parameter. Usually it has one of two physically motivated forms,  $\Delta = \Delta_1 = |\mathbf{k}_T|/\mu$  and  $\Delta = \Delta_2 = |\mathbf{k}_T|/(|\mathbf{k}_T| + \mu)$ , which reflects the strong ordering (SO) or angular ordering (AO) conditions for parton emissions at the last evolution step. The

<sup>2</sup>The analytical expressions for TMDs were obtained [51] in both differential and integral definitions of the KMR/WMR approach.

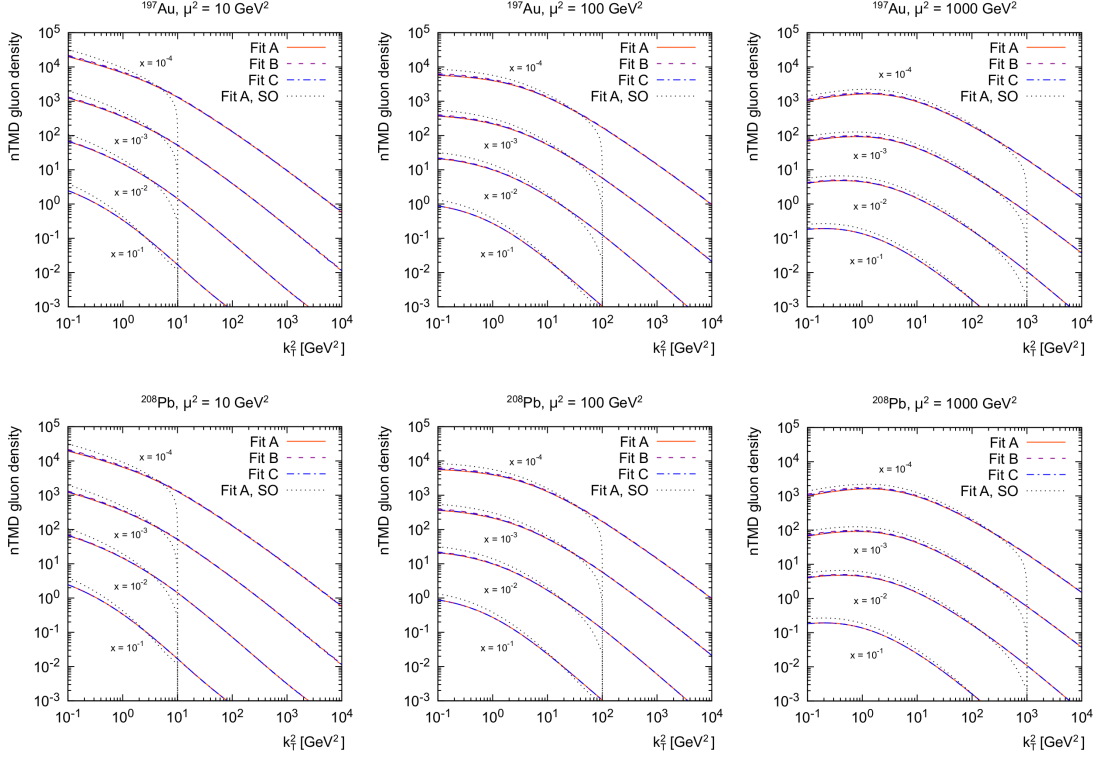


Figure 1: nTMD gluon densities in  $^{197}\text{Au}$  and  $^{208}\text{Pb}$  calculated as functions of  $\mathbf{k}_T^2$  for several  $x$  and  $\mu^2$  using the angular ordering and strong ordering conditions. Different scenarios for their nuclear dependence, namely, Fit A, B and C, described in the text (see also [52]), are applied.

Sudakov form factors  $T_a(\mathbf{k}_T^2, \mu^2)$  give the probability of evolving from a scale  $\mathbf{k}_T^2$  to a scale  $\mu^2$  without parton emission:

$$\ln T_a(\mathbf{k}_T^2, \mu^2) = - \int_{\mathbf{k}_T^2}^{\mu^2} \frac{d\mathbf{p}_T^2}{\mathbf{p}_T^2} \frac{\alpha_s(\mathbf{p}_T^2)}{2\pi} \sum_b \int_0^{1-\Delta} dz z P_{ba}(z). \quad (16)$$

The analytical expressions for  $T_a(\mathbf{k}_T^2, \mu^2)$  can be found in [73]. It is important to note that the KMR/WMR prescription is only correct at  $\mathbf{k}_T^2 > \mu_0^2$ , where  $\mu_0^2 \sim 1 \text{ GeV}^2$  is the minimum scale where the perturbative QCD is still applicable. At low  $\mathbf{k}_T^2$  special model assumptions, usually related with the overall normalization of the TMDs/nTMDs, are necessary (see [31, 32, 69, 72]). However, in our consideration, these parton densities are well defined in the whole  $\mathbf{k}_T^2$  range since "frozen" treatment of the QCD coupling in the infrared region is applied, where  $\alpha_s(\mu^2) \rightarrow \alpha_s(\mu^2 + M_\rho^2)$  with  $M_\rho \sim 1 \text{ GeV}$ . Such treatment was used in all the fits [51, 52] and results in a good description of the data on structure function  $F_2(x, Q^2)$  and  $F_2^A(x, Q^2)$ , or rather their ratios.

In Fig. 1 we show the nTMD gluon distributions in  $^{197}\text{Au}$  and  $^{208}\text{Pb}$  calculated as functions of  $\mathbf{k}_T^2$  for several values of  $x$  and scale  $\mu^2$  using mentioned above scenarios for nuclear dependence, Fit A, B and C (see also [52]). These results were obtained with the angular and strong ordering conditions. As it was expected, the nTMDs extend into the  $\mathbf{k}_T^2 > \mu^2$  region in the case of angular ordering and vanish at large  $\mathbf{k}_T^2$  in the case of strong ordering condition. We find that different assumptions on the  $A$ -dependence of rescaling parameters have only weak impact on predicted nTMDs. In fact, results of calculations

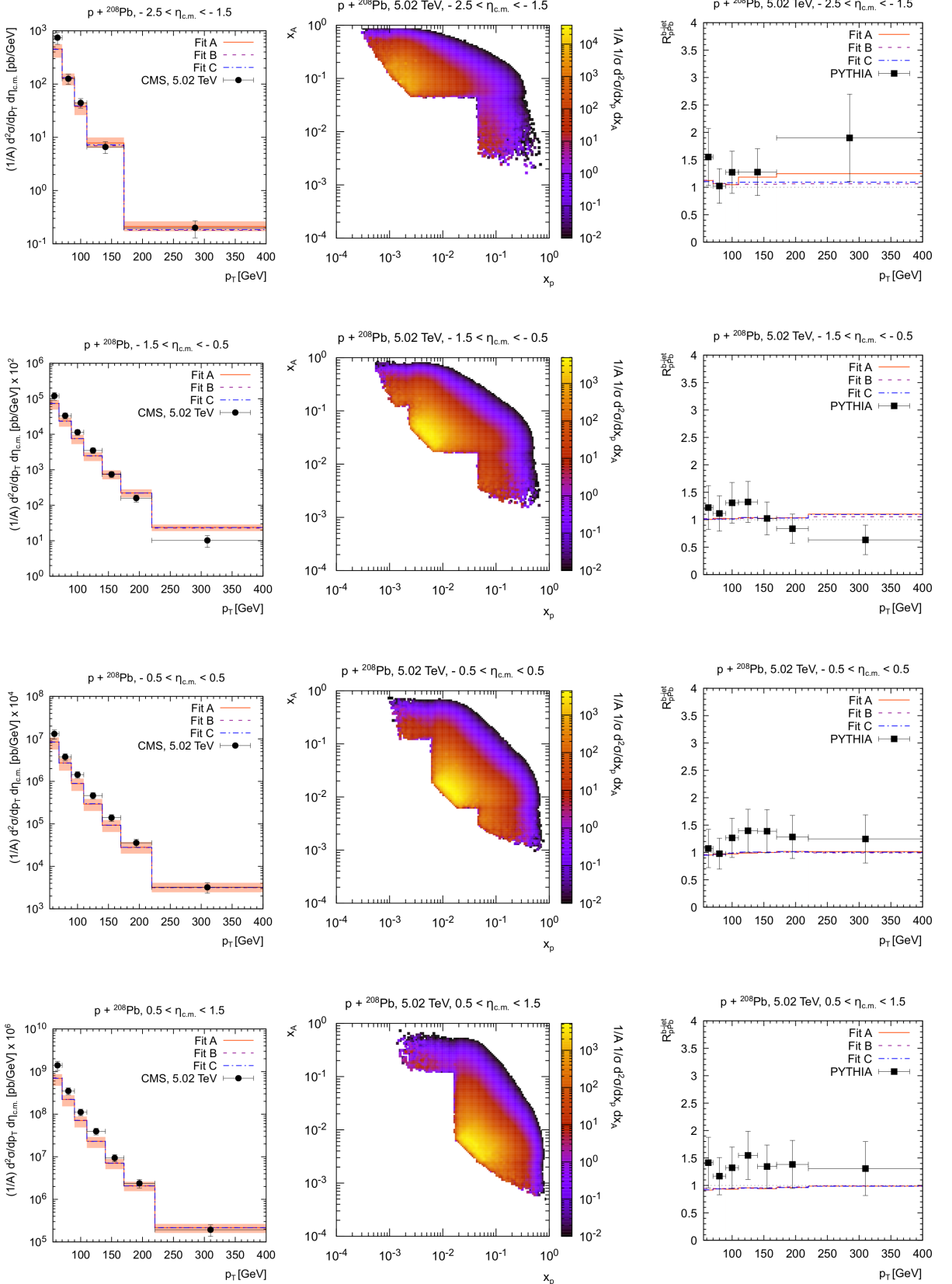


Figure 2: Transverse momentum spectra of inclusive  $b$ -jet production compared to CMS data [57] (left panels), normalized double differential cross sections as functions of longitudinal momentum fractions of proton,  $x_p$ , and nucleus,  $x_A$  (center panels), and nuclear modification factors  $R_{p\text{Pb}}^{b\text{-jet}}$  (right panels). Different scenarios for their nuclear dependence, namely, Fit A, B and C, described in the text (see also [52]), with AO condition are applied. The uncertainty band is shown for Fit A results only.

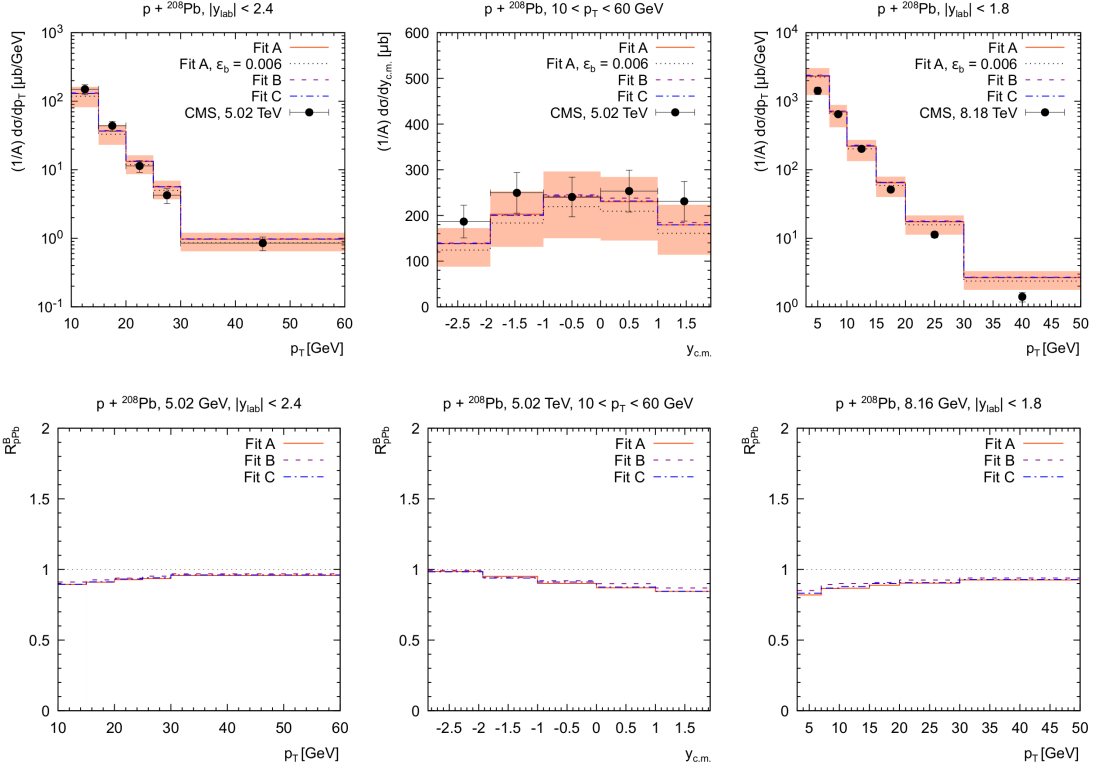


Figure 3: Transverse momentum and rapidity spectra of inclusive  $B^+$ -jet production compared to CMS data [58, 59] (upper panels) and corresponding nuclear modification factors  $R_{pPb}^{B^+}$  (lower panels). Different scenarios for their nuclear dependence, namely, Fit A, B and C, described in the text (see also [52]), with AO condition are applied. The uncertainty band is shown for Fit A results only.

based on Fit A, B and C are very close to each other in a wide kinematical range.

As it has already been noted above, here we will test the obtained nTMDs with the data on beauty production in proton-lead collisions at the LHC. We strictly follow the previous evaluations [41, 74] done in the High Energy Factorization [2], or  $k_T$ -factorization [3] approach and employ the FFNS scheme with  $N_f = 4$ . In such a way, the main contribution to beauty production comes from the off-shell gluon-gluon fusion subprocess  $g^* + g^* \rightarrow b + \bar{b}$ , which is implemented into the Monte-Carlo event generator PEGASUS [56]. The contribution from the quark-induced process is of almost no importance because of comparatively low quark densities. The cross section is given by the convolution of the TMD gluon densities in a proton and/or nuclei and off-shell (dependent on the transverse momenta of incoming partons) hard scattering amplitudes (see [6, 7] for more information). Note that MC generator PEGASUS was used, in particular, by the ATLAS [75, 76] and ALICE [77, 78] Collaborations in the analyses of their data on heavy quark bound states production at the LHC.

We consider the latest measurements of inclusive  $b$ -jet and  $B^+$  meson production performed by the CMS Collaborations at  $\sqrt{s} = 5.02$  and  $8.16$  TeV [57–59]. The CMS data on  $b$ -jet transverse momentum spectra [57] refer to the transverse momentum range  $55 < p_T < 400$  GeV and were obtained at  $\sqrt{s} = 5.02$  TeV in four different proton-lead center-of-mass pseudorapidity subdivisions, namely,  $-2.5 < \eta_{c.m.} < -1.5$ ,  $-1.5 < \eta_{c.m.} < -0.5$ ,  $-0.5 < \eta_{c.m.} < 0.5$  and  $0.5 < \eta_{c.m.} < 1.5$ . Note that the positive rapidities refer to the beam orientation where the proton is moving toward positive  $z$  direction. The

transverse momentum and rapidity distributions of  $B^+$  mesons have been measured at  $10 < p_T < 60$  GeV,  $|y_{\text{lab}}| < 2.4$  and  $\sqrt{s} = 5.02$  TeV [58]. Very recently, first data on  $B^+$  meson production at  $\sqrt{s} = 8.16$  TeV have been reported in the kinematical range  $3 < p_T < 50$  GeV and  $|y_{\text{lab}}| < 1.8$  [59]. In the present calculations, we identify the produced  $b$  quark with the beauty jet. To convert  $b$  quarks to  $B^+$  mesons, we apply standard Peterson fragmentation function with shape parameter  $\epsilon_b = 0.003$ , which is often used in the pQCD calculations. We set  $m(b) = 4.183$  GeV,  $m(B^+) = 5.279$  GeV and branching ratios  $B(b \rightarrow B^+) = 0.408$  [79]. Following to fits [51, 52], the calculations were made with the one-loop formula for QCD coupling  $\alpha_s$  with  $\Lambda_{\text{QCD}}^{(4)} = 118$  MeV.

Our predictions are shown in Fig. 2 and Fig. 3. In Fig. 2 we plot the transverse momentum spectra of inclusive  $b$ -jet production compared to the CMS data [57], normalized double differential cross sections as functions of longitudinal momentum fractions  $x_p$  and  $x_A$  (carried by the gluons originated from proton and nuclear target, respectively) and corresponding nuclear modification factors  $R_{p\text{Pb}}^{b\text{-jet}} = 1/A(d\sigma_{p\text{Pb}}^{b\text{-jet}}/dp_T)/(d\sigma_{pp}^{b\text{-jet}}/dp_T)$ , where  $A = 208$  is the number of nucleons in the Pb nucleus. The results of calculations for  $B^+$  meson production are shown in Fig. 3. The AO condition is applied everywhere and calculations are done in the each of pseudorapidity subdivisions considered in the CMS analysis. Solid, dashed and dash-dotted histograms corresponds to the central results for different scenarios of nuclear dependence, where we fixed both renormalization and factorization scales at their default values,  $\mu_R^2 = \mu_F^2 = p_T^2$ . The shaded bands correspond to scale uncertainties of the calculations, shown for Fit A scenario. These uncertainties have been estimated in a standard way, by varying the scales  $\mu_R$  and  $\mu_F$  by a factor of 2 around their default values. We find that our predictions based on Fit A, Fit B and Fit C parametrizations of nuclear dependence are rather close to each other and consistent with the data within the theoretical and experimental uncertainties. However, overall agreement achieved in rear kinematical region (negative  $\eta_{\text{c.m.}}$ ) is somewhat better than in the forward one. In fact, our results tend to slightly underestimate the CMS data at forward rapidities. It is clear that main contribution in this region comes from events where essentially small- $x_A$  region of nuclear target  $A$  is probed (see Fig. 2). Thus, the observed difference may indicate that the nuclear shadowing effects, which manifest themselves mainly at low  $x_A$ , could be overestimated in our analysis. Another point is related with effects of parton showers and/or hadronization in final state. However, it is difficult to give a definite conclusion due to relatively large theoretical uncertainties of our calculations and shortage of the nuclear experimental data used in the determination of rescaling parameters (see also [52]). Moreover, additional higher-order pQCD contributions (not covered by the non-collinear pQCD evolution encoded in the TMDs/nTMDs) also could play a role (see, for example, [80, 81] and references therein). An accurate addressing to all of these issues needs a dedicated study and is out of the present consideration.

It was already pointed out that special kinematical cuts on the final state provide possibilities to achieve the wanted region of  $x_A$  [53]. So, with increasing  $\eta_{\text{c.m.}}$  the peak of the normalized cross section  $1/\sigma d^2\sigma/dx_p dx_A$  shifts gradually to lower  $x_A$  values, which immediately reflects in the predicted nuclear medium modification factor  $R_{p\text{Pb}}^{b\text{-jet}}$  (see Fig. 2). In particular, our calculations show sizeable antishadowing and shadowing effects with  $R_{p\text{Pb}}^{b\text{-jet}} \sim 1.1 - 1.2$  and  $R_{p\text{Pb}}^{b\text{-jet}} \sim 0.9 - 1.0$  in the rear and forward kinematical regions, respectively. Similar values are obtained for  $B^+$  mesons (see Fig. 3). Thus, we demonstrate that one can investigate the nuclear medium effects by applying the different cuts on the final states produced in the high energy  $pA$  collisions. This is important to precise determination of the partonic content of nuclei, where there are a lot of differences among

predictions from different groups<sup>3</sup>.

Finally, to investigate the dependence of our predictions on the  $b \rightarrow B^+$  fragmentation function, we repeated the calculations with the shifted value of the Peterson shape parameter,  $\epsilon_b = 0.006$ . The results of our calculations are shown in Fig. 3 by dotted histograms. We find that the obtained cross sections are somewhat smaller for larger  $\epsilon_b$  values. However, these predictions lie within the estimated theoretical uncertainties.

To conclude, we have evaluated nTMDs at the leading order in QCD coupling using the popular Kimber-Martin-Ryskin/Watt-Martin-Ryskin approach. The calculations have been based on a rescaling model with taking into account Fermi motion effects and global analysis of available DIS data for different nuclear targets. The obtained nTMDs have been successfully tested with latest CMS data on beauty production in proton-lead collisions collected at  $\sqrt{s} = 5.02$  and  $8.16$  TeV. We predict the corresponding nuclear medium modification factors to be about of  $0.8 - 1.2$ . Specially we have highlighted the possibility to investigate the nuclear modification of parton densities by applying different cuts on the final states produced in the  $pA$  collisions. It can be important for forthcoming studies of lepton-nucleus, proton-nucleus and nucleus-nucleus interactions at modern and future colliders, where nuclear parton dynamics could be examined directly.

Note that the consideration can be improved by taking into account effects of parton showers and/or higher-order pQCD corrections. We plan to investigate these issues in ensuing studies.

*Acknowledgements.* We thank S.P. Baranov, M.A. Malyshev and H. Jung for their interest, very important comments and remarks. We are also grateful to A.Yu. Alekseenko for testing the TMDs used in this work. This research has been carried out at the expense of the Russian Science Foundation grant No. 25-22-00066, <https://rscf.ru/en/project/25-22-00066/>.

## References

- [1] V.N. Gribov, L.N. Lipatov, Sov. J. Nucl. Phys. **15**, 438 (1972);  
L.N. Lipatov, Sov. J. Nucl. Phys. **20**, 94 (1975);  
G. Altarelli, G. Parisi, Nucl. Phys. B **126**, 298 (1977);  
Yu.L. Dokshitzer, Sov. Phys. JETP **46**, 641 (1977).
- [2] S. Catani, M. Ciafaloni, F. Hautmann, Nucl. Phys. B **366**, 135 (1991);  
J.C. Collins, R.K. Ellis, Nucl. Phys. B **360**, 3 (1991).
- [3] L.V. Gribov, E.M. Levin, M.G. Ryskin, Phys. Rep. **100**, 1 (1983);  
E.M. Levin, M.G. Ryskin, Yu.M. Shabelsky, A.G. Shuvaev, Sov. J. Nucl. Phys. **53**, 657 (1991).
- [4] E.A. Kuraev, L.N. Lipatov, V.S. Fadin, Sov. Phys. JETP **44**, 443 (1976);  
E.A. Kuraev, L.N. Lipatov, V.S. Fadin, Sov. Phys. JETP **45**, 199 (1977);  
I.I. Balitsky, L.N. Lipatov, Sov. J. Nucl. Phys. **28**, 822 (1978).
- [5] M. Ciafaloni, Nucl. Phys. B **296**, 49 (1988);  
S. Catani, F. Fiorani, G. Marchesini, Phys. Lett. B **234**, 339 (1990);  
S. Catani, F. Fiorani, G. Marchesini, Nucl. Phys. B **336**, 18 (1990);  
G. Marchesini, Nucl. Phys. B **445**, 49 (1995).

---

<sup>3</sup>The pseudorapidity-integrated value predicted by the PYTHIA event generator [82] is  $R_{p\text{Pb}}^{b\text{-jet}} = 1.22 \pm 0.15$  (stat. + syst. exp.)  $\pm 0.27$  (syst. PYTHIA), see [57]. To compare with our results, in Fig. 2 we show the PYTHIA predictions (taken from [57]) separately for each rapidity subdivision.

- [6] A.V. Lipatov, S.P. Baranov, M.A. Malyshev, *Phys. Part. Nucl.* **55**, 256 (2024).
- [7] R. Angeles-Martinez, A. Bacchetta, I.I. Balitsky, D. Boer, M. Boglione, R. Boussarie, F.A. Ceccopieri, I.O. Cherednikov, P. Connor, M.G. Echevarria, G. Ferrera, J. Grados Luyando, F. Hautmann, H. Jung, T. Kasemets, K. Kutak, J.P. Lansberg, A. Lelek, G.I. Lykasov, J.D. Madrigal Martinez, P.J. Mulders, E.R. Nocera, E. Petreska, C. Pisano, R. Placakyte, V. Radescu, M. Radici, G. Schnell, I. Scimemi, A. Signori, L. Szymanowski, S. Taheri Monfared, F.F. Van der Veken, H.J. van Haevermaet, P. Van Mechelen, A.A. Vladimirov, S. Wallon, *Acta Phys. Polon. B* **46**, 2501 (2015).
- [8] EMC Collaboration, *Phys. Lett. B* **123**, 275 (1983).
- [9] M. Arneodo, *Phys. Rept.* **240**, 301 (1994).
- [10] P.R. Norton, *Rept. Prog. Phys.* **66**, 1253 (2003).
- [11] S. Malace, D. Gaskell, D.W. Higinbotham, I.C. Clöt, *Int. J. Mod. Phys. E* **23**, 1430013 (2014).
- [12] E.V. Shuryak, *JETP* **47**, 212 (1978).
- [13] J.C. Collins, M.J. Perry, *Phys. Rev. Lett.* **34**, 1353 (1975).
- [14] M. Hirai, S. Kumano, T.-H. Nagai, *Phys. Rev. C* **70**, 04495 (2004).
- [15] M. Hirai, S. Kumano, T.-H. Nagai, *Phys. Rev. C* **76**, 065207 (2007).
- [16] K.J. Eskola, *Nucl. Phys. A* **910**, 163 (2013).
- [17] K.J. Eskola, P. Paakkinen, H. Paukkunen, C.A. Salgado, *Eur. Phys. J. C* **82**, 413 (2022).
- [18] R.A. Khalek, R. Gauld, T. Giani, E.R. Nocera, T.R. Rabemananjara, J. Rojo, *Eur. Phys. J. C* **82**, 507 (2022).
- [19] A.W. Denniston, T. Jezo, A. Kusina, N. Derakhshanian, P. Duwentaster, O. Hen, C. Keppel, M. Klasen, K. Kovarik, J.G. Morfin, K.F. Muzakka, F.I. Olness, E. Pisetzky, P. Risse, R. Ruiz, I. Schienbein, J.Y. Yu, *Phys. Rev. Lett.* **133**, 152502 (2024).
- [20] R. Wang, X. Chen, Q. Fu, *Nucl. Phys. B* **920**, 1 (2017).
- [21] E. Blanco, A. van Hameren, H. Jung, A. Kusina, K. Kutak, *Phys. Rev. D* **100**, 054023 (2019).
- [22] S.A. Kulagin, R. Petti, *Nucl. Phys. A* **765**, 126 (2006).
- [23] S.A. Kulagin, R. Petti, *Phys. Rev. C* **90**, 045204 (2014).
- [24] R.L. Jaffe, F.E. Close, R.G. Roberts, G.G. Ross, *Phys. Lett. B* **134**, 449 (1984); O. Nachtmann, H.J. Pirner, *Z. Phys. C* **21**, 277 (1984); F.E. Close, R.L. Jaffe, R.G. Roberts, G.G. Ross, *Phys. Rev. D* **31**, 1004 (1985).
- [25] F.E. Close, R.G. Roberts, G.G. Ross, *Phys. Lett. B* **129**, 346 (1983); R.L. Jaffe, *Phys. Rev. Lett.* **50**, 228 (1983).
- [26] A.M. Stasto, K. Golec-Biernat, J. Kwiecinski, *Phys. Rev. Lett.* **86**, 596 (2001).

- [27] N. Armesto, C.A. Salgado, U.A. Wiedemann, Phys. Rev. Lett. **94**, 022002 (2005).
- [28] G.R. Boroun, B. Rezaei, Pramana J. Phys. **98**, 161 (2024).
- [29] A.V. Lipatov, G.I. Lykasov, M.A. Malyshev, Phys. Rev. D **112**, 014025 (2025).
- [30] R.L. Jaffe, arXiv:2212.05616 [hep-ph].
- [31] M.A. Kimber, A.D. Martin, M.G. Ryskin, Phys. Rev. D **63**, 114027 (2001).
- [32] G. Watt, A.D. Martin, M.G. Ryskin, Eur. Phys. J. C **31**, 73 (2003).
- [33] A.D. Martin, M.G. Ryskin, G. Watt, Eur. Phys. J. C **66**, 163 (2010).
- [34] R. Maciula, R. Pasechnik, A. Szczurek, Phys. Rev. D **106**, 054018 (2022).
- [35] A. Cisek, A. Szczurek, Phys. Rev. D **103**, 114008 (2021).
- [36] K. Golec-Biernat, L. Motyka, T. Stebel, Phys. Rev. D **103**, 034013 (2021).
- [37] M. Modarres, M.R. Masouminia, R. Aminzadeh-Nik, H. Hosseinkhani, N. Olanj, Phys. Rev. D **94**, 074035 (2016).
- [38] B. Guiot, A. van Hameren, Phys. Rev. D **104**, 094038 (2021).
- [39] F.E. Barattini, C.O. Dib, B. Guiot, arXiv:2501.17662 [hep-ph].
- [40] S. Rezaie, K. Azizi, Phys. Lett. B **868**, 139787 (2025).
- [41] A.V. Lipatov, M.A. Malyshev, A.V. Kotikov, X. Chen, Phys. Lett. B **850**, 138486 (2024).
- [42] G. Cvetic, A.Yu. Illarionov, B.A. Kniehl, A.V. Kotikov, Phys. Lett. B **679**, 350 (2009).
- [43] A.Yu. Illarionov, A.V. Kotikov, S.S. Parzycki, D.V. Peshekhonov, Phys. Rev. D **83**, 034014 (2011).
- [44] A.V. Kotikov, B.G. Shaikhatdenov, P.M. Zhang, Phys. Rev. D **96**, 114002 (2017).
- [45] A.V. Kotikov, A.V. Lipatov, B.G. Shaikhatdenov, P. Zhang, JHEP **02**, 028 (2020).
- [46] A.V. Kotikov, A.V. Lipatov, P. Zhang, Phys. Rev. D **104**, 054042 (2021).
- [47] A.V. Kotikov, G. Parente, Nucl. Phys. B **549**, 242 (1999).
- [48] A.Yu. Illarionov, A.V. Kotikov, G. Parente, Phys. Part. Nucl. **39**, 307 (2008).
- [49] L. Mankiewicz, A. Saalfeld, T. Weigl, Phys. Lett. B **393**, 175 (1997).
- [50] N.A. Abdulov, A.V. Kotikov, A.V. Lipatov, Particles **5**, 535 (2022).
- [51] A.V. Kotikov, A.V. Lipatov, Phys. Rev. D **111**, 094009 (2025).
- [52] A.V. Kotikov, A.V. Lipatov, Chin. Phys. **50**, 034109 (2026).
- [53] S.P. Baranov, H. Jung, A.V. Lipatov, M.A. Malyshev, Eur. Phys. J. C **77**, 2 (2017).
- [54] X. Dong, Y.-J. Lee, R. Rapp, Ann. Rev. Nucl. Part. Sci. **69**, 417 (2019).

[55] L. Apolinario, Y.-J. Lee, M. Winn, *Prog. Part. Nucl. Phys.* **127**, 103990 (2022).

[56] A.V. Lipatov, M.A. Malyshev, S.P. Baranov, *Eur. Phys. J. C* **80**, 330 (2020).

[57] CMS Collaboration, *Phys. Lett. B* **754**, 59 (2016).

[58] CMS Collaboration, *Phys. Rev. Lett.* **116**, 032301 (2016).

[59] CMS Collaboration, *Phys. Rev. Lett.* **134**, 111903 (2025).

[60] A. Bodek, J.L. Ritchie, *Phys. Rev. D* **23**, 1070 (1981).

[61] L.L. Frankfurt, M.I. Strikman, *Nucl. Phys. B* **181**, 22 (1981).

[62] L.D. McLerran, R. Venugopalan, *Phys. Rev. D* **49**, 2233 (1994);  
L.D. McLerran, R. Venugopalan, *Phys. Rev. D* **49**, 3352 (1994).

[63] A.H. Mueller, *Nucl. Phys. A* **724**, 223 (2003).

[64] K. Rummukainen, H. Weigert, *Nucl. Phys. A* **739**, 183 (2004).

[65] Y.V. Kovchegov, *Phys. Rev. D* **61**, 074018 (2000).

[66] E. Levin, K. Tuchin, *Nucl. Phys. B* **573**, 833 (2000).

[67] E.P. Segarra, T. Jezo, A. Accardi, P. Duwentäster, O. Hen, T.J. Hobbs, C. Keppel, M. Klasen, K. Kovarik, A. Kusina, J.G. Morfin, K.F. Muzakka, F.I. Olness, I. Schienbein, J.Y. Yu, *Phys. Rev. D* **103**, 114015 (2021).

[68] M. Klasen, H. Paukkunen, *Ann. Rev. Nucl. Part. Sci.* **74**, 49 (2024).

[69] K. Golec-Biernat, A.M. Stasto, *Phys. Lett. B* **781**, 633 (2018).

[70] B. Guiot, *Phys. Rev. D* **101**, 054006 (2020).

[71] R.K. Valeshabadi, M. Modarres, *Eur. Phys. J. C* **82**, 66 (2022).

[72] B. Guiot, *Phys. Rev. D* **107**, 014015 (2023).

[73] G.R. Boroun, Phuoc Ha, A.V. Kotikov, A.V. Lipatov, arXiv:2510.14678 [hep-ph].

[74] H. Jung, M. Kraemer, A.V. Lipatov, N.P. Zotov, *JHEP* **01**, 085 (2011);  
H. Jung, M. Kraemer, A.V. Lipatov, N.P. Zotov, *Phys. Rev. D* **85**, 034035 (2012).

[75] ATLAS Collaboration, *Phys. Rept.* **1116**, 57 (2025).

[76] ATLAS Collaboration, *Eur. Phys. J. C* **84**, 169 (2024).

[77] ALICE Collaboration, *JHEP* **03**, 190 (2022).

[78] ALICE Collaboration, *Eur. Phys. J. C* **81**, 1121 (2021).

[79] PDG Collaboration, *Phys. Rev. D* **110**, 030001 (2024).

[80] S.P. Baranov, A.V. Lipatov, A.A. Prokhorov, X. Chen, *Eur. Phys. J. C* **84**, 348 (2024).

[81] A.A. Prokhorov, S.P. Baranov, A.V. Lipatov, M.A. Malyshev, X. Chen, *Phys. Rev. D* **112**, 114022 (2025).

[82] T. Sjöstrand, S. Mrenna, P. Skands, *JHEP* **05**, 026 (2006).